Drops distributions and flux measurements in sprays using the phase Doppler technique

by

I. V. Roisman and C. Tropea

Technische Universität Darmstadt

Fachgebiet Strömungslehre und Aerodynamik

Petersenstraße 30, 64287 Darmstadt; Germany

ABSTRACT

The subject of the present investigation is the measurement of the flux and concentration of drops in sprays using the phase Doppler technique. One important issue is the difference between the illuminated volume and the detection volume, the detection volume being a function of particle size, photodetector location and specifications, signal detection criteria, etc. A further consideration is the count error due to multiple particles in the volume. A statistical correction for this effect is introduced and shown to be already significant in relatively sparse sprays. Comparisons between various estimators and a simple patternator confirm the improvements of the new estimators.

As an illustration of the improvements achieved, measurements downstream of a simple pressure atomizer are considered. In Fig. 1 the mass flux in the main spray direction (x) calculated by commercial software and by the present model, including the multiple drop consideration and the reference area expression, are compared with the results of measurements by a patternator at different downstream distances l from the nozzle. The agreement of the present model with the data obtained by the collector is good, even at points where the flux and the relative signal presence are high. The model used in the commercial software does not take into account the presence of multiple drop signals and as a result underestimates the mass flux at small distances from the nozzle, where the drop concentration is high.

The model is based on the assumption that the drops in the spray are distributed randomly and thus the probability of two or more drops in the probe volume can be described by the Poisson distribution. Once this probability is estimated from the measured data resident times, the total drop counts can be adjusted accordingly, assuming no correlation between occurrence probability in the volume and particle size. As an example of the significance of this consideration, if the measured residence times amount to 30% of the total measurement duration, already 50% more droplets are present than are registered as signals. This greatly influences the derived fluxes.

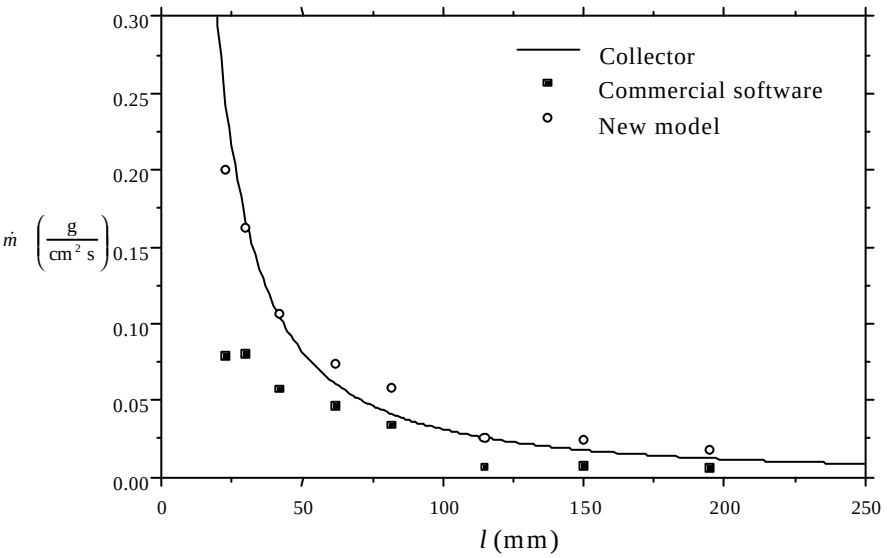

Fig. 1: Comparison of the mass flux calculated by commercial software and by the present model with the results of measurements by the patternator.

The present model also allows computation of fluxes in arbitrary directions, even when the main flow direction of the spray is not aligned with the x-axis of the phase Doppler system. The phase Doppler measurements are in good agreement with the measurements using the tube collector, both for inclined impinging sprays and for an inclined collector plane. This allows investigations in regions of the spray, where strong variations of the velocity directions can be expected, for example near the wall or in the region of interaction of two sprays.

1. Introduction

Among the parameters important for the investigation of atomization and spray transport processes such as evaporation, drop coagulation or wall impact, the local fluxes and concentration of drops are likely the most important. The phase-Doppler technique is a suitable instrument to provide this information, however it is legitimate to question the achievable measurement accuracy and whether this accuracy is sufficient for a given purpose.

A general expression for the flux vector V_{gi} of an arbitrary, extensive scalar property q of drops in a spray can be written as

$$\dot{\mathbf{Q}} = \frac{1}{T}\sum_{i=1}^{N_{sv}} \frac{h_{vi}\, q_i}{A_{gi}(D_i, g_i)} \mathbf{e}_{gi} \quad , \tag{1}$$

where T is the measurement time, N_{sv} is the number of validated signals, $\frac{pr_p}{12}$ is the diameter of the i-th drop, $\mathbf{e}_{gi}$ is the unit vector in the direction of its motion, A_{gi} is the reference area of the measurement volume, g_i is the particle trajectory angle to be defined below and h_{vi} is a correction factor accounting for count errors due to multiple particles occurring in the measurement volume or for non-validation of particles. The factor h_{vi} is introduced for the first time in this study and will be described below in more detail.

Examples of q are:

$$q_i = 1, \qquad \text{for the number flux,} \tag{2a}$$

$$q_i = \frac{pr}{6} D_i^3 \quad , \qquad \text{for the mass flux,} \tag{2b}$$

$$q_i = \frac{pr}{12} D_i^3 u_i^2 \, , \qquad \text{for the kinetic energy flux,} \tag{2c}$$

where r is the particle density and u_i is the particle velocity.

The concentration C_q of the property q is a scalar and can be expressed in the following form

$$C_q = \frac{1}{T}\sum_{i=1}^{N_{sv}} \frac{h_{vi}\, q_i}{A_g(D_i, g_i)\, u_i} = \frac{1}{T}\sum_{i=1}^{N_{sv}} \frac{h_{vi}\, t_i\, q_i}{V_g(D_i, g_i)} \quad , \tag{3}$$

where V_{gi} is the volume of the measurement volume and t_i is the residence time of the particle.

It is well known that flux and concentration measurements using the phase Doppler technique can exhibit large errors, as has been shown through comparisons with the integral flux of a spray (Dullenkopf et al., 1998). Several sources of error in the mass flux measurement have been identified, including the trajectory effect or Gaussian beam effect (Saffaman, 1986, Gréhan et al., 1991, Sankar et al., 1992), the slit effect (Durst et al., 1994, Xu and Tropea, 1994), as well as errors due to non-validated droplets and in estimating the size dependent area over which the flux is measured. Certainly errors can also occur due to obscuration, either in the transmitting beams, which lead to local wave front distortion in the measurement volume, or in the receiving line of sight. Although these effects have not yet been systematically considered, a lower signal-to-noise ratio and hence a higher variance for all signal parameter estimations can be expected.

In Dullenkopf et al., 1998 the results of mass flux measurements using the models of Tropea et al., 1996 and Sommerfeld and Qiu, 1995 and various configurations of the phase-Doppler technique (phase-Doppler particle analyzer (PDPA), Dual-mode PDA and Qiu and Sommerfeld – PDA (QS-PDA)) were compared with data obtained by a patternator, consisting of a set of tubes collecting water. The volume flux in the patternator was calculated by measuring the collected volume of water, the elapsed time and the sampling area. It was shown that in the cases of relatively low density sprays, the DualPDA (the data rate was 6 kHz) and the QS-PDA (the data rate was 9 kHz) agree well with the results of the mass flux obtained by the patternator. In the cases of higher density sprays (data rates of 35 and 30 kHz, respectively) the error becomes more significant. In Dullenkopf et al., 1998 it is further noted that a possible error could be caused by the presence of two or more drops in the probe volume simultaneously, which is one of the subjects of the present work.

In Edwards and Marx, 1992 the influence of the possible presence of multiple particles in the probe volume on the measurements of the size distribution function and on the fluxes is analyzed. The statistics of the particles in the detection

volume, assumed to be an ellipsoid, is described using the Poisson distribution. The probability that a given particle will be validated includes two parts: the probability that at the initial instant when the particle reaches the detection volume, the volume is free from other particles; and the probability that during the transit time of the given particle, no other particle enters the detection volume. It is shown that in the case of relatively dense sprays, the influence of the multiple particles in the probe volume can however be significant.

The main subject of the present paper is to develop a theoretical model of measuring the flux using the phase-Doppler technique, accounting for the probability of two or more drops in the probe volume simultaneously and to validate the model experimentally. As in Dullenkopf et al., 1998, the proposed model approximates the detection volume by a cylinder of the diameter d_t truncated by the projected slit of width L_s under the receiver off-axis angle f. The method of estimating the diameter $d_t(D)$ of the detection volume accounts for the fact that the projected area depends both on the drop diameter D and on the direction of its motion. Then the drop occurrence probability and the ratio N_d/N_s of the number of drops to the number of signals is estimated as a function of the measured signal rate. Subsequently, the values for the drop size distribution and for the flux are corrected due to the effect of N_d/N_s.

2. DESCRIPTION of the MODEL

2.1 Geometry of the detection volume

A brief summary of the detection volume geometry is given in this section with complete details available in Tropea et al., 1996, Roisman et al., 1999, Zhang and Ziada, 2000. Consider a Cartesian coordinate system with the base vectors $\{\mathbf{e}_x, \mathbf{e}_y\}$ fixed at the center of the detection volume (Fig. 2a). The detection volume is represented by the intersection of a prolate ellipsoid (approximated by a cylinder of effective diameter d_t depending on the drop diameter D_i) with the projected slit of width L_s (Fig. 2b). This diameter depends on the trigger value used to detect the signal as well as parameters such as laser power, photodetector voltage, system gain, etc., all of which will be assumed to be constant. Note also that this volume may be significantly displaced from the illumination volume, as described in (Araneo et al., 2000), although this displacement is of only secondary importance for the present analysis. Denote $\mathbf{e}_s$ as the unit vector normal to the slit. The slice created by the slit intersecting with the cylinder has elliptical surfaces of axes d_t and $d_t/\sin f$ with an area of

$$A_s = \frac{p\, d_t^{\,2}}{4 \sin f} \quad . \tag{4}$$

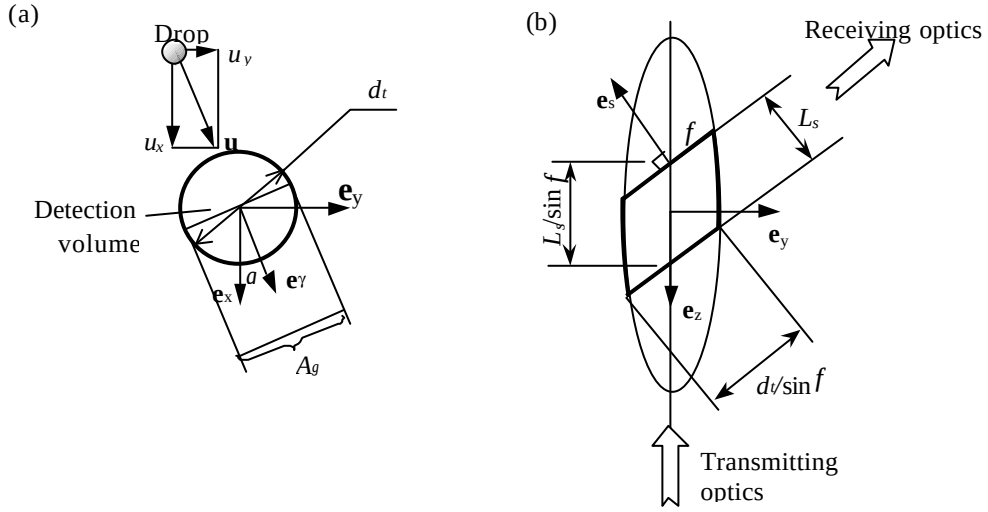

Fig. 2: Geometry of a detection volume. (a) – view on the plane {x, y}, (b) – view on the plane {y, z}.

Consider the unit vector $\mathbf{e}_\gamma$ forming the angle g with $\mathbf{e}_x$ (Fig. 2a). As was determined in (Roisman et al., 1999) and (Zhang and Ziada, 2000) the area of projection of the measured volume to the plane normal to $\mathbf{e}_\gamma$ is

$$A_g^* = \frac{d_t L_s}{\sin f} + A_s \left| \mathbf{e_s} \bullet \mathbf{e}_? \right| \quad . \tag{5}$$

One of the conditions of drop validation is that the signal envelope crosses the amplitude trigger value two times – at the beginning and at the end of the burst. This condition is not satisfied by drops piercing the slices. Moreover, when a drop pierces the slice, the signal corresponding to reflected light may becomes dominant/significant (slit effect) and the drop may not be validated due to the low signal-to-noise ratio. This rejection is even more reliable if additional measures are taken, such as with a dual-mode optical arrangement or by demanding a certain correlation between signal amplitude and measured size. Therefore the reference area A_g of validated drops can be obtained by excluding the areas of projections of the ellipses (corresponding to the slices) from the projected area A_g^*

$$A_g = \frac{d_t L_s}{\sin f} - A_s \left| \mathbf{e_s} \bullet \mathbf{e}_? \right| \quad . \tag{6}$$

Such an area estimate has not yet been used with the phase Doppler technique and represents one of the novel suggestions of the present work.

Combining Eqns. (4) – (6) yields an expression for the projected area A_g in the following form

$$A_g = \frac{d_t L_s}{\sin f} - \frac{p\, d_t^2 \left|\sin g\right|}{4 \tan f} \quad , \qquad \sin g = \frac{u_y}{\sqrt{u_x^2 + u_y^2}} \tag{7a,b}$$

The reference volume V_g of the detection volume depends on the direction of motion of the drop and can be expressed in the form:

$$V_{gs} = d_t^3 \int_0^1 \int_0^{\sqrt{1-x'^2}} \sqrt{1 - y'^2 \frac{\cos^2 f}{\sin^2 g}}\; dy'\, dx' \approx \frac{p d_t^2 L_s}{4 \sin f} - \frac{p d_t^3 \left|\sin g\right|}{6 \tan f} \quad , \tag{8}$$

where axis x' is parallel to $\mathbf{e}_g$ and axis y' is normal to the unit vectors $\mathbf{e}_g$ and $\mathbf{e}_z$.

2.2 Estimation of the Number of Detected Drops

Presence of drops in the probe volume

Assume that the arrival time of each drop is distributed randomly but uniformly (stationarity) within the observation time interval T. Consider N_s signals detected from N_d drops crossing the probe in the time interval T. Due to the possible overlapping of signals from two or more drops simultaneously in the measurement volume the number N_s is in general smaller than N_d.

Denote t_i as the residence time of the i-th drop, s_j is the duration of the j-th signal. The probability of the i-th drop being in the measurement volume at a certain instant of time is t_i / T. Let l be the sum of these probabilities over all the N_d drops occuring in the time period T:

$$l = \frac{1}{T} \sum_{i=1}^{N_d} t_i \quad . \tag{9}$$

The probability $p(n;\, l)$ that at a certain instant we can observe exactly n drops simultaneously can be described by the Poisson distribution (Feller, 1968)

$$p(n;\, l) = e^{-l} \frac{l^n}{n!} \quad . \tag{10}$$

whereas the probability $p(0;\, l)$ that at a certain instant we observe no drop can be measured as

$$p(0;l) = 1 - \frac{1}{T}\sum_{i=1}^{N_s} s_i \qquad (11)$$

Equations (9)-(11) yield the following expression for the *occurrence probability* l (Poisson parameter) of drops in the volume

$$l = -\ln(1-e), \qquad e = \frac{1}{T}\sum_{i=1}^{N_s} s_i, \qquad (12a,b)$$

where e is the *relative time interval* with signals present.

Calculation of the number of drops

The goal now is to estimate from these measurable parameters the ratio of the number of drops to the number of detected signals. The signals from drop d_i and drop d_j overlap when

$$t_i \in \left\lfloor t_j - t_i, t_j + t_j \right\rfloor, \qquad (13)$$

where t_i and t_j are the time instants at which the i-th and j-th droplets are first detected (see Fig. 3).

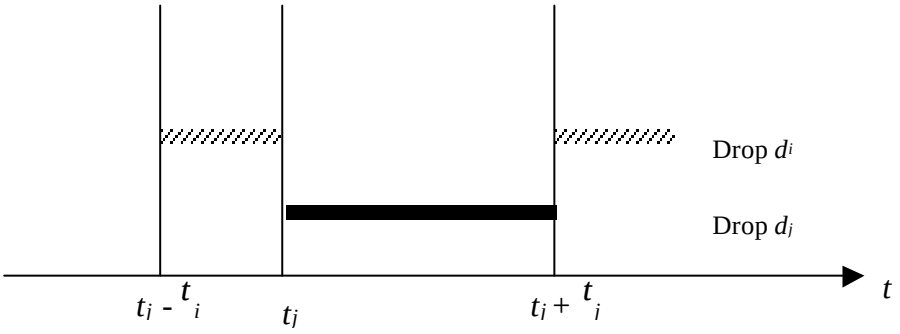

Fig. 3: Timing diagram illustrating two limiting cases of no drop overlap between drops d_i *and* d_j.

Therefore, the probability that the signals from the drops d_i and d_j overlap is

$$p_{ij} = \frac{t_i + t_j}{T}. \qquad (14)$$

Using Eqns. (9) and (14) and noting that $N_d >> 1$, the probability that the signal from drop d_i overlaps with any other drop crossing the detection volume in time T is

$$p_i = \sum_{j=1,\ j\neq i}^{N_d} p_{ij} \approx \frac{N_d t_i}{T} + l. \qquad (15)$$

The probability that the signal from drop d_i will overlap exactly with n other drops can be found using the Poisson distribution

$$P_i(n) = e^{-p_i}\frac{p_i^n}{n!}. \qquad (16)$$

The probability of one registered signal arising from four drops is of order $O(p_i^3)$ and will be neglected in the present analysis. The probability $p(3, l)$ that at a certain instant we register signals from three drops simultaneously is also assumed negligibly small. The number N_s of registered signals can be estimated as a sum of the number of single signals and the sum of probabilities for each drop to be at the beginning of the multiple signals. To begin, the case that drop d_i generates a signal arising from only one drop is given by the probability $P_i(0)$ of no overlap. Next, the probability $P_i(1)$ that the given drop d_i overlaps exactly with one other drop must be halved to account for the fact that the given drop

can occur either at the beginning or end of the multiple drop signal. Therefore, the number of signals can be expressed in the following form:

$$N_s = \sum_{i=1}^{N_d} \mathrm{P}_i(0) + \frac{1}{2}\sum_{i=1}^{N_d} \mathrm{P}_i(1) \ . \tag{17}$$

Assuming p_i <<1 yields

$$e^{-p_i} \approx 1 - p_i + \frac{p_i^2}{2} + \mathrm{O}(p_i^3) \ . \tag{18}$$

Using Eqns. (15) - (18) and neglecting terms of order higher than $\mathrm{O}(p_i^3)$ yields the following expression for the number of registered signals:

$$N_s = N_d - \frac{1}{2}\sum_{i=1}^{N_d} p_i \ . \tag{19}$$

Equation (19) is evaluated with the help of Eqns. (9) and (15) to obtain

$$N_s = N_d(1-l) \ . \tag{20}$$

Now, knowing the number N_s of detected signals and the relative time interval with signals present e, the ratio of the number of drops to the number of signals in the time interval T can be estimated using Eq. (12) as

$$\frac{N_d}{N_s} = \frac{1}{1+\ln(1-e)} \ . \tag{21}$$

The RHS of Eq. (21) is valid only for $e < 1 - e^{-1} \approx 0.632$ (see Fig. 4). At higher values of e the number of signals corresponding to three or more simultaneous drops become significant, which is not taken into account in the present model.

Correction factor to the number of drops

The probability that the drop residence period in the detection volume will overlap with another drop's residence period will be directly proportional to the residence time. Consider n_{dk} drops of the residence time class t_k. The average number n_{sk} of signals corresponding to these drops can be found by the method analogous to that used in deriving Eq. (17)

$$n_{sk} = n_{dk}\left[\mathrm{P}_k(0) + \frac{1}{2}\mathrm{P}_k(1)\right] \ . \tag{22}$$

The ratio of the sum of residence times of drops in the class k to the total duration of corresponding signals does not depend on t_i, therefore

$$\frac{n_{dk}\, t_k}{n_{sk}\, s_k} = \frac{l}{e} \ , \tag{23}$$

where s_k is the average duration of the signals corresponding to the drops in the residence time class k. Substituting expression (22) into Eq. (23) yields

$$\left[\mathrm{P}_k(0) + \frac{1}{2}\mathrm{P}_k(1)\right] s_k = \frac{e}{l} t_k \ . \tag{24}$$

With the help of Eq. (16), Eq. (24) can be written in the form

$$s_k \left[1 + \frac{p_k(t_k)}{2}\right] \exp\left[-p_k(t_k)\right] = \frac{e}{l} t_k \ . \tag{25}$$

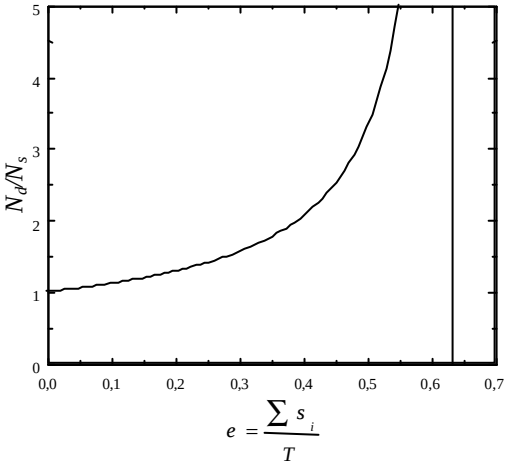

Fig. 4: The ratio of the number of drops to the number of detected signals as a function of the relative time interval with signals e.

Substituting expressions (15) and (18) into Eq. (25) and neglecting terms of order $O(p_i^3)$ yields

$$\frac{t_k}{s_k} = \frac{2-l}{2\frac{e}{l} + \frac{N_d}{T} s_k} \cdot \tag{26}$$

Now the expression (26) is substituted into (23) to obtain the following expression for the average number of drops h_k corresponding to one signal of the duration s_k

$$h_k = \frac{n_{dk}}{n_{sk}} = \frac{1}{2-l}\left(2 + \frac{l\, N_d}{e\, T} s_k\right) \cdot \tag{27}$$

Not all detected signals are validated by the software. We assume that the probability of each drop to be non-validated is uniform (does not depend on its diameter or velocity) and introduce a constant correction factor *r* such that

$$r \sum_{i=1}^{N_{sv}} h_i = N_d \ , \tag{28}$$

where N_{sv} is the number of validated signals, which is smaller than the total number N_s of detected signals. Using Eqns. (27) and (28) in Eq. (20) the following expression for *r* is obtained

$$r = \frac{2-l}{\left(2\frac{N_{sv}}{N_d} + l\,\frac{e_v}{e}\right)} \ , \tag{29}$$

where the relative signal presence e_v of validated signals is defined by

$$e_v = \sum_{i=1}^{N_{sv}} \frac{s_i}{T} \tag{30}$$

Now, the average number h_{vi} of drops corresponding to each validated signal can be found using Eqns. (27) - (30) as

$$h_{vi} = r h_i = \left(2 + \frac{l}{e}\frac{N_d}{T} s_i\right) \Big/ \left(2\frac{N_{sv}}{N_d} + l\,\frac{e_v}{e}\right) \cdot \tag{31}$$

The value of h_{vi} is used as a correction factor in Eq. (1) for the of flux calculations or in Eq. (2) for the concentration calculations.

3. EXPERIMENTAL INVESTIGATION

The experimental set-up is shown schematically in Fig. 5. Water is supplied from the pressure vessel (1) to the spray nozzle (2). The volume flux of the spray at a given point is measured using the collector (3), consisting of a glass tube with an inner diameter of 8.8 mm. The mass flux was calculated by multiplying the value of the collected volume of water by its density and dividing by the elapsed time. The flowmeter (4) allows variation of the spray flux.

Two components (axial and transverse) of the drop velocity and the drop diameter are measured using a phase Doppler instrument (Dantec Measurement Technology), including a transmitting (5) and a receiving (6) optics, photomultipliers (7), the processor (8) and a personal computer (9). Signals from the processor are monitored on an oscilloscope (10). The probe volume is positioned using a traversing system (11).

Measurements of the flux by the phase Doppler and by the collector were performed simultaneously. Flux was measured by the phase Doppler at 3 points, each 1mm above the collector (see Fig. 5b) and then averaged over the area of the collector. The flux was calculated using Eq. (1) with the quantity q defined in Eq. (2b), the reference area A_{gi} was calculated using (7a) and the correction factor h_{vi} estimated using Eq. (31). The experiments were performed at different distances from the nozzle and used various configurations of the phase Doppler technique. The list of experiments and optical configurations is given in Table 1.

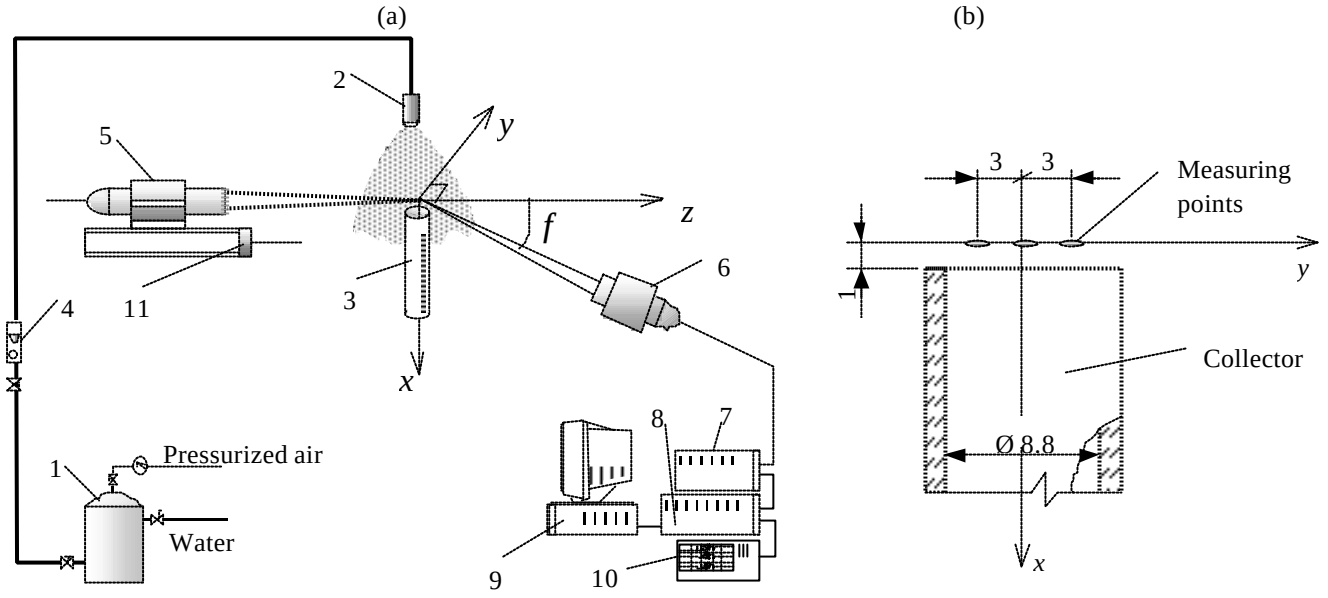

Fig. 5: (a) – Overview of experiment; (b) - Location of the measuring points relative to the collector (dimensions given in millimeters).

Table 1: List of experiments

	Exp. 1	Exp. 2	Exp. 3
Optical set-up	Dual PD	Dual PD	Fiber PD
Lens focal length:			
Transmitting, mm	310	600	600
Receiving, mm	400	160	400
Scattering angle, degrees	30	30	30
Projected slit width, mm	0.413	0.165	0.413
Nominal illuminated volume, mm^3	0.0146	0.0220	0.0551
Nominal diameter of the illuminated volume, mm	0.151	0.292	0.292

An example of a correlation of the droplet size D and the axial component u_x of drop velocity for the spray is shown in Fig. 6. The main flow of the spray is directed along the vertical x-axis. The intensity of the gray color in the figure corresponds to the value of the probability density function $f_x^{[p]}(D,u_x)$ of the drops crossing the plane normal to the vertical x-axis. The possible correlation indicates that the spray was issuing into stagnant surroundings and being decelerated from its exit velocity. The smaller droplets react more quickly due to their lower inertia. Over 90% of all droplets were lees than 50 mm in diameter, which means that even in Experiment 1 the droplets were less than 1/3 of the measurement volume. Thus the Gaussian beam effect is not expected to be significant.

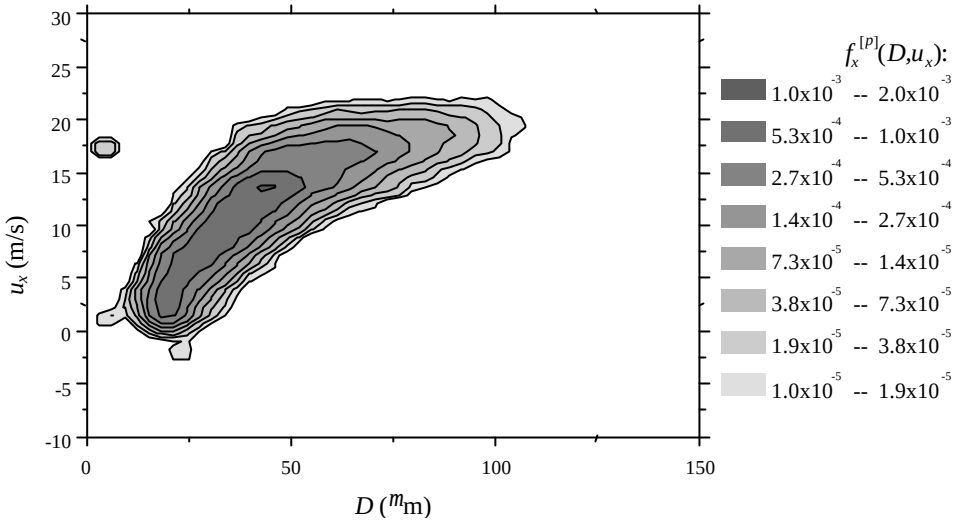

Fig. 6: Contour plot of the probability density function of the drops by the diameter D and the axial component of velocity u_x.

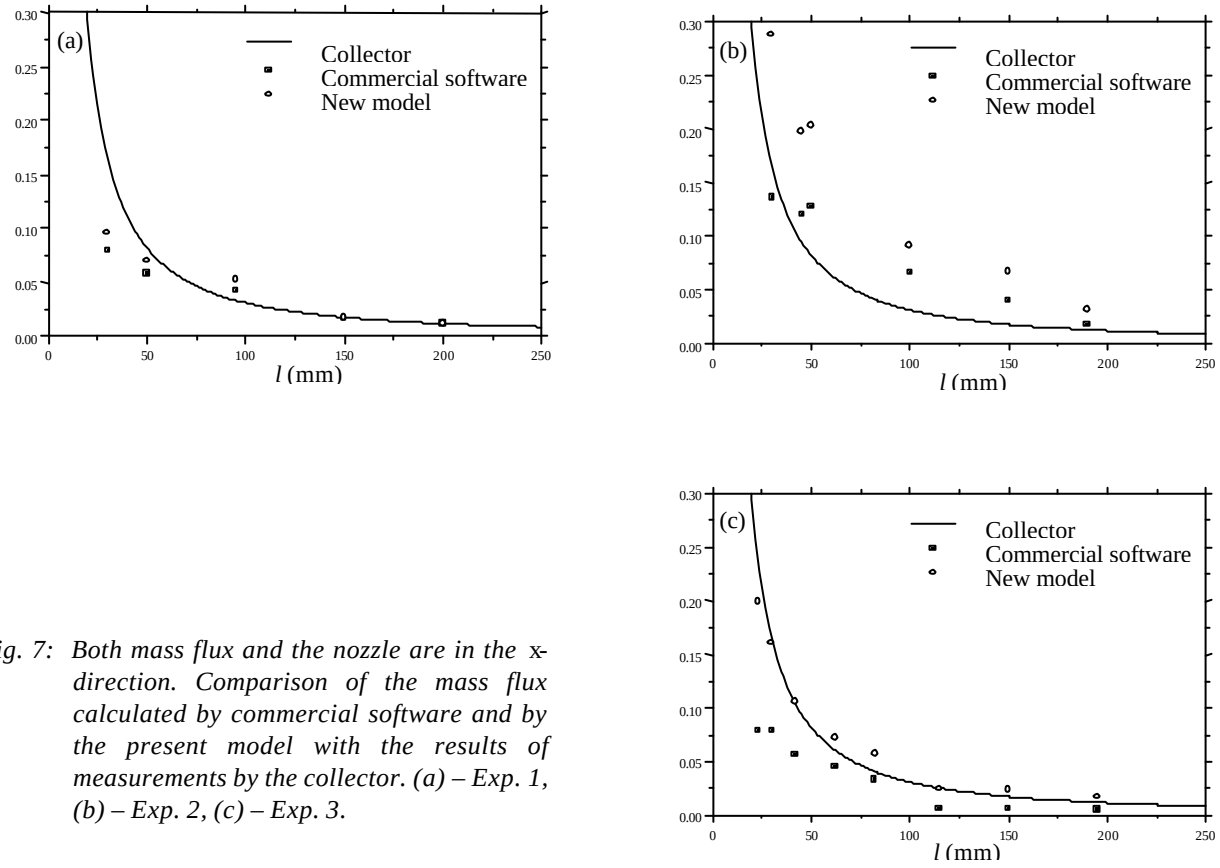

Fig. 7: Both mass flux and the nozzle are in the x-direction. Comparison of the mass flux calculated by commercial software and by the present model with the results of measurements by the collector. (a) – Exp. 1, (b) – Exp. 2, (c) – Exp. 3.

In Fig. 7 the mass flux in the *x*-direction calculated by the commercial software and by the present model are compared with the results of measurements by the collector. The nozzle was directed vertically in the *x*-direction (see Fig. 5a). In experiments 1 and 2 a dual mode phase Doppler instrument was used. The results of experiment 1 show good agreement between both the commercial software and the newly proposed model with those of the collector. In experiment 2 (Fig. 7b) both models overestimate the mass flux. In this experiment the diameter of the illuminated volume d_t exceeds significantly the projected slit width L_s=165 μm and the slit effect influences the results of the flux measurements. In experiments 1 and 3, where the diameter-to-length ratio of the illuminated volume is relatively small (reducing the influence

of the slit effect) the agreement of the present model with the data obtained by the collector is good, even at points where the flux and the relative signal presence are high (see Fig. 7a,c). The model used in the commercial software does not take into account the presence of multiple drop signals and as a result underestimates the mass flux at small distances from the nozzle where the drop concentration is high.

The commercial software assumes that the spray flow is directed in the *x*-axis. In the next set of experiments the axis of the nozzle formed various angles b with the *x*-axis. In Figs. 8, 9 and 10 the results of the measurements of the mass flux are shown as a function of the angle b. In Fig. 8 the mass flux is in the *x*-direction $\dot{m}_x$, in Fig. 9 the mass flux $\dot{m}_a$ at an angle $a = 40°$ with the *x*-axis is measured, and in Fig. 10 the mass flux in the *y*-direction $\dot{m}_y$ measured by the collector are compared with the results of calculations based on the conventional model (using expression (4) for the projected area and not accounting for the possibility of two drops being in the measurement volume instantaneously) and with the results of the newly proposed model. The present model of calculation of the flux is in better agreement with the measurements of the collector.

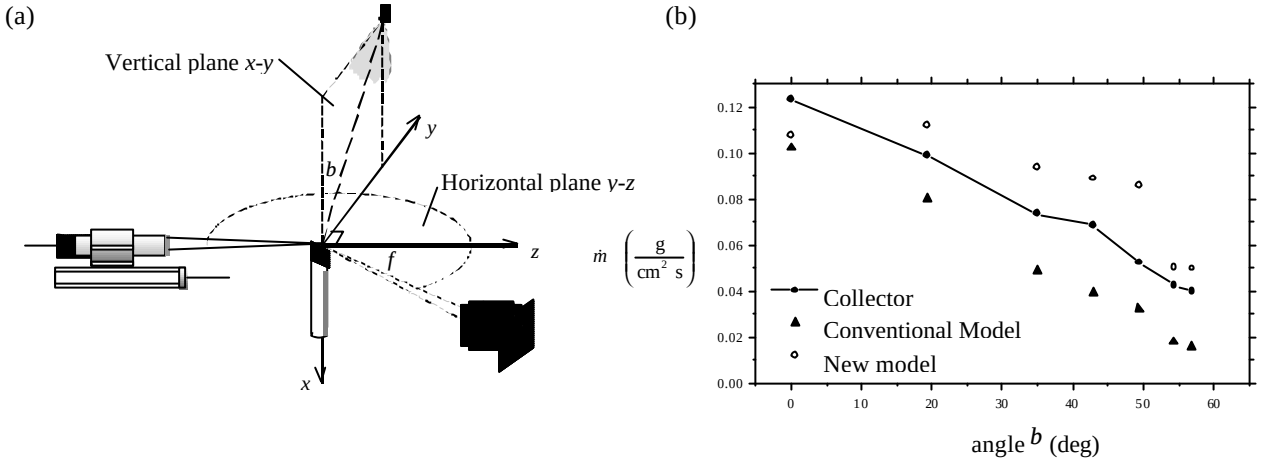

Fig. 8: Mass flux in the x-direction, the nozzle axis is orientated at an angle β to the x-axis. (a) – Configuration of the set-up. (b) - Comparison of the mass flux measured by the collector, calculated by the conventional model and calculated by the present model. Configuration of phase Doppler instrument corresponds to Exp. 1 in Table 1.

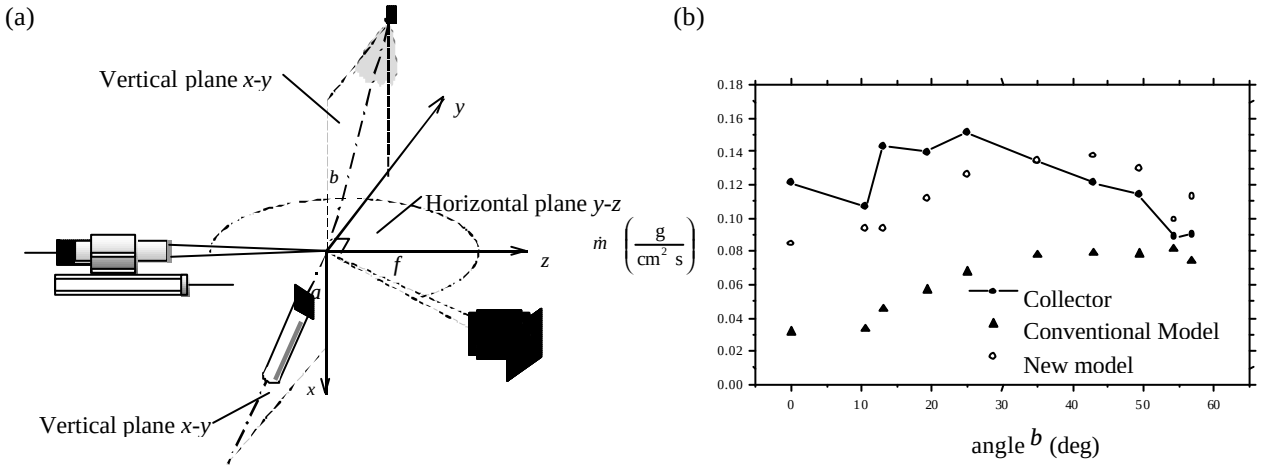

Fig. 9: Mass flux at the angle a = 40° with the x-direction, the nozzle axis is oriented at the angle b to the x-axis. (a) – Configuration of the set-up. (b) - Comparison of the mass flux measured by the collector, calculated by the conventional model and calculated by the present model. Configuration of phase Doppler instrument corresponds to Exp. 1 in Table 1.

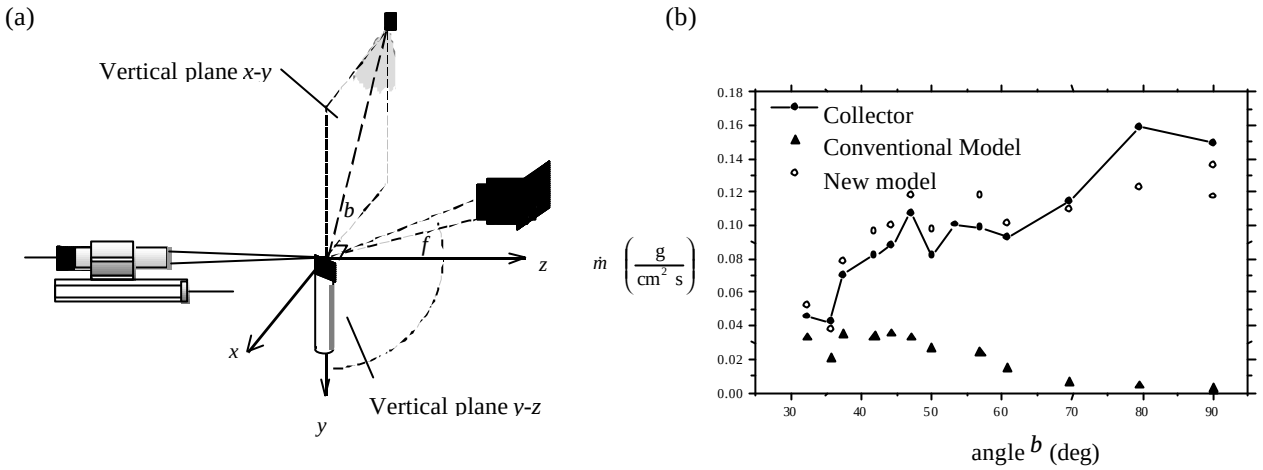

Fig. 10 Mass flux in the y-direction, the nozzle axis is orientated at an angle b to the x-axis. (a) – Configuration of the set-up. (b) - Comparison of the mass flux measured by the collector, calculated by the conventional model and calculated by the present model. Configuration of phase Doppler instrument corresponds to Exp. 1 in Table 1.

4. CONCLUSIONS

The model developed in the present work accounts for the complex geometry of the measurement volume and for the probability of two or more drops in the probe volume simultaneously. The model is based on the assumption that the drops in the spray are distributed randomly and thus the probability of two or more drops in the probe volume can be described by the Poisson distribution. It has been shown that for relatively dense sprays the influence of the overlapping of the signals of two or more drops on the measured flux becomes significant. When the relative time interval with signals e is small (<0.2) estimations of the mass flux in the x-direction based on the present model and commercial software are in good agreement and reasonably accurate, except for the case when the projected slit width is too thin (is of order of the drop diameter).

The present model is in good agreement with the measurements with the collector, even for calculations of the fluxes in arbitrary directions and when the main flow of the spray is not directed in the x-axis. The latter allows one to investigate regions where the main flow of the spray changes its direction, for example near the wall or in the region of interaction of two sprays.

ACKNOWLEDGEMENTS

I. V. Roisman would like to thank the Alexander von Humboldt Foundation for the financial support of his stay in Darmstadt. The research was in part supported by the Deutsche Forschungsgemeinschaft through grant Tr 194/10-3.

REFERENCES

Araneo, L., Damaschke, N., Tropea, C. (2000). "Measurement and Prediction of the Gaussian Beam Effect in the Phase Doppler Technique, 10th Int. Symp. on Appl. of Laser Techn. to Fluid Mech., Lisbon, 10-13 July.

Dullenkopf, K., Willmann, M., Wittig, S., Schöne, F., Stieglmeier, M., Tropea, C., Mundo, C. (1998). "Comparative Mass Flux Measurements in Sprays Using a Patternator and the Phase-Doppler Technique", Part. Part. Syst. Charact., 15, pp. 81-89.

Durst, F., Tropea, C., Xu, T.-H. (1994). "The Slit Effect in Phase Doppler Anemometry", Proc. 2nd Int. Conf. On Fluid Dyn. Meas. And its Appl., Beijin.

Edwards, C. F. and Marx, K. D. (1992). "Analysis of The Ideal Phase-Doppler System: Limitations Imposed by the Single-Particle Constraint", Atomization and Sprays, 2, pp. 319-366.

Feller, W. (1968). "An Introduction to Probability Theory and its Applications", 3rd ed., John Wiley & Sons. New York, Chichester, Brisbane, Toronto. Volume I, p. 154.

Gréhan, G., Gouesbet, G.,. Naqwi, A, Durst, F. (1991). "Evaluation of a Phase Doppler System Using Generalized Lorenz-Mie Theory", Proc. Int. Conf. On Multiphase Flows '91, Tsukuba, Japan, pp. 291-296.

Roisman, I. V., Araneo, L., Marengo, M., Tropea, C. (1999). "Evaluation of Drop Impingement Models: Experimental and Numerical Analysis of a Spray Impact", Proc. 15th Annual Conference on Liquid Atomization and Spray Systems, ILASS-Europe, Toulouse.

Saffman, M. (1986). "The use of polarized light for optical particle sizing", Proc. Anemometry in Fluid Mechanics-III, LADOAN – Instituto Superior Técnico, Lisbon, pp. 387-398.

Sankar, S. V., Inenaga, A., Bachalo, W. D. (1992). "Trajectory Dependent Scattering in Phase Doppler Interferometry: Minimizing and Eliminating Sizing Errors", Proc. 6th Int. Symp. Of Appl. Of Laser Tech. To Fluid Mechanics, LADOAN, Lisbon, pp. 75-89.

Sommerfeld, M. and Qiu, H.-H. (1995). "Particle Concentration Measurements by Phase-Doppler Anemometry in Complex Dispersed Two-Phase Flows", Exp. in Fluids, 18, pp. 187-198.

Tropea, C.,. Xu, T.-H., Onofri, F., Grehan, G., Haugen, P., Stieglmeier, M. (1996). "Dual-Mode Phase-Doppler Anemometer", Part. Part. Syst. Charact., 13, pp. 165-170.

Xu, T.-H., Tropea, C. (1994). "Improving the performance of two-component phase Doppler anemometers", Meas. Sci. Technol. 5 pp. 969-975.

Zhang, Zh., Ziada, S. (2000). "PDA Measurements of Droplet Size and Mass Flux in the Three-Dimensional Atomization Region of Water Jet in Air Cross-Flow", Experiments in Fluids, 28, pp. 29-35.